

Synthesis, structure and dielectric properties of $(1-x)$ $[0.9\text{BiFeO}_3-0.1\text{DyFeO}_3]-x\text{PbTiO}_3$ pseudo-binary ceramics

Jian Zhuang^a, Ling Chen^a, Wei Ren^{a,*}, Zuo-Guang Ye^{a,b,*}

^aElectronic Materials Research Laboratory, Key Laboratory of the Ministry of Education & International Center for Dielectric Research, Xi'an Jiaotong University, Xi'an 710049, China

^bDepartment of Chemistry and 4D LABS, Simon Fraser University, Burnaby, British Columbia, Canada, V5A 1S6

Available online 16 October 2012

Abstract

In order to develop multiferroics with large magnetization and polarization, we have prepared a series of $(1-x)[0.9\text{BiFeO}_3-0.1\text{DyFeO}_3]-x\text{PbTiO}_3$ [BDF- x PT] solid solution ceramics by solid state reaction. X-ray diffraction reveals that, with the increase of PbTiO_3 concentration, the solid solution transforms from a rhombohedral to a tetragonal phase with the presence of a morphotropic phase boundary (MPB) region located at $0.28 \leq x \leq 0.40$ at room temperature, in which the rhombohedral, tetragonal and orthorhombic phases coexist. The temperature dependence of the dielectric permittivity indicates that the Curie temperature decreases with the increasing amount of PbTiO_3 . Based upon the structural analysis and dielectric characterization, a preliminary phase diagram for the BDF- x PT pseudo-binary system has been proposed. It is found that the ceramics of compositions around the MPB exhibits much better dielectric properties with dielectric constant of the BDF-0.37PT ceramics reaching 459 at 1 kHz, confirming the beneficial effects of the MPB on the dielectric performance.

© 2012 Elsevier Ltd and Techna Group S.r.l. All rights reserved.

Keywords: Sintering; X-ray methods; Dielectric properties; Perovskites

1. Introduction

In the past few years, a great deal of attention has been paid on multiferroics materials which possess simultaneously ferroelectricity and (anti)ferromagnetism (and also ferroelasticity). As a promising multiferroic material for practical applications, BiFeO_3 (BF) shows a high Curie temperature ($\sim 850^\circ\text{C}$) and a large spontaneous polarization ($90\text{--}100\text{ }\mu\text{C}/\text{cm}^2$) [1–5], as well as improved magnetization by doping with Ba, Pb and Ga [6]. However, there are severe obstacles to overcome before BF can be used in device applications, such as the difficulties in preparing the pure perovskite phase and the large leakage current due to the charge transfer between the mixed valence ions of Fe^{3+} and Fe^{2+} [3–5]. Moreover, the weak ferromagnetism arising from the Dzyaloshinskii–Moriya

(D–M) interaction between the Fe^{3+} ions limits the strength of magnetoelectric coupling in BiFeO_3 [2].

Chemical modifications by doping, substitution or forming solid-solution with other ferroelectric materials have proved to be important and effective methods to stabilize the perovskite structure of BF, reduce the leakage current and improve the physical properties [7–12]. Among those approaches, the $\text{BiFeO}_3\text{--PbTiO}_3$ solid solution has been extensively studied, which is formed in pure perovskite phase and displays good dielectric, ferroelectric and magnetic properties [7–10]. The solid solution of $(1-x)\text{BiFeO}_3\text{--}x\text{DyFeO}_3$ appears to be another interesting system which exhibits a large remnant polarization and an improved magnetism because Dy^{3+} is a magnetic rare-earth ion [11]. With the increase of DyFeO_3 concentration, a morphotropic phase transition from perovskite rhombohedral (R3c) to orthorhombic orthoferrite (Pnma) was observed at x around 0.1. In order to obtain a stable perovskite phase, improved dielectric, ferroelectric and ferromagnetic properties, and ultimately, enhanced magnetoelectric coupling, we have prepared in this work the

*Corresponding authors at: Electronic Materials Research Laboratory, Key Laboratory of the Ministry of Education & International Center for Dielectric Research, Xi'an Jiaotong University, Xi'an 710049, China. Tel.: +86 29 82668679; fax: +86 29 82668794.

E-mail addresses: wren@mail.xjtu.edu.cn (W. Ren), zye@sfu.ca (Z.-G. Ye).

$(1-x)[0.9\text{BiFeO}_3-0.1\text{DyFeO}_3]-x\text{PbTiO}_3$ pseudo-binary solid solution ceramics and investigated their structure and dielectric properties.

2. Experimental

A series of $(1-x)[0.9\text{BiFeO}_3-0.1\text{DyFeO}_3]-x\text{PbTiO}_3$ (BDF- x PT) ($x=0, 0.1, 0.2, \dots$, and 0.9) ceramics were prepared by solid state reaction and sintering method. The raw materials of Bi_2O_3 ($\geq 99\%$), Fe_2O_3 ($\geq 99\%$), Dy_2O_3 (99.9%), PbO ($\geq 99\%$) and TiO_2 ($\geq 98\%$) were weighed in the stoichiometric proportions. To compensate the evaporation of Bi_2O_3 , an excess amount of Bi_2O_3 (2 mol%) was added to the starting reactants in the bismuth-rich compositions ($x=0, 0.1, 0.2, \dots$, and 0.9). After mixing with dilute alcohol, ball milling for 7 h, the mixed powder was dried and pressed into pellets with a diameter of $\Phi=25$ mm. The pellets were calcined at 850°C for 2 h in an alumina crucible. The calcined samples were ground thoroughly once again, mixed with 5% polyvinyl alcohol (PVA) and then pressed into pellets with $\Phi=12$ mm. The pellets were subsequently heated at 700°C for 1 h to eliminate the PVA binder and sintered at higher temperatures, from 1000°C to 1100°C , for 2 h, depending on composition. To characterize the electric properties, the ceramic samples were polished and covered with silver paste on the both circular surfaces as electrodes.

The structure and phases were examined by X-ray diffraction (XRD, Rigaku D/Max-2400) with $\text{CuK}\alpha$ radiation. The lattice parameters were refined from the XRD profiles by using the JADE software (Materials Data, Inc.). The dielectric properties were measured at room temperature in a wide frequency range from 1 kHz to 10 MHz using a precision impedance analyzer (4294A, Agilent). The temperature variation of the dielectric properties were measured up to 900°C , *i.e.*, above the Curie temperature, at selected frequencies.

3. Results and discussion

The samples are named after their compositions, *e.g.*, PT10 stands for $0.9(0.9\text{BiFeO}_3-0.1\text{DyFeO}_3)-0.1\text{PbTiO}_3$, and so on. After sintering, most samples reach a relative density of 90%. However, PT00 and PT10 samples exhibit a much lower density with roughness surface because of the severe evaporation of Bi_2O_3 . As we known, the pure lead titanate ceramic is hard to densify and very easy to crack. As the amount of PT increases from PT37 to PT90, the density of samples decreases. It is also worth mentioning that PT40 ceramic is easy to break into pieces or powder after sintering because of the large tetragonality and the coexistence of two or three phases in this composition near the morphotropic phase boundary (MPB). In addition, the PT37 ceramic exhibits the highest relative density of 98%.

Fig. 1 shows the XRD patterns of the BDF- x PT ceramics (in ground powders). For $x \leq 0.25$, the samples

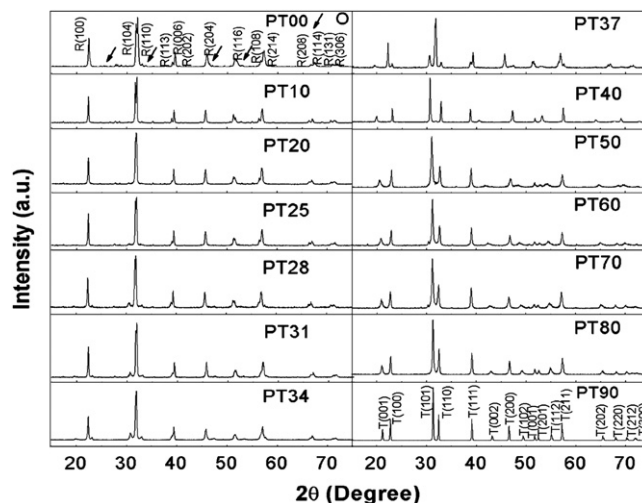


Fig. 1. XRD patterns of the ground powders of the BDF- x PT ceramics sintered at 1000°C – 1100°C .

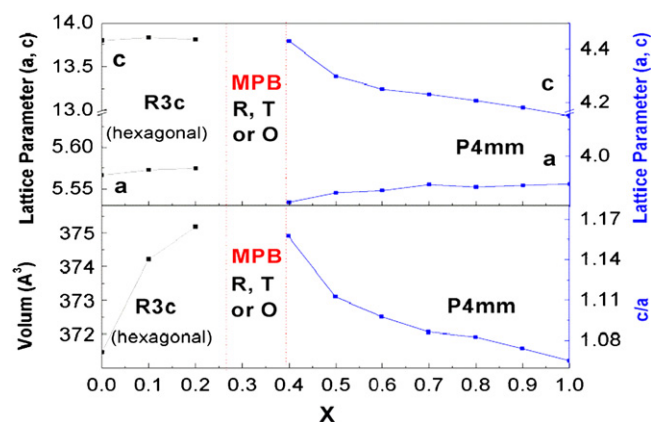


Fig. 2. Variation of the lattice parameters, volume and c/a ratio for the BDF- x PT ceramics.

mainly exhibit a rhombohedral (R3c) structure with a small amount of the orthorhombic phase (as indicated by the arrows), which is consistent with the literature[11], since $0.9\text{BF}-0.1\text{DF}$ is close to the MPB composition of the BF-DF solid solution. As the amount of lead titanate increases, the tetragonal (P4mm) phase starts to appear in PT28, and consequently, three phases, the rhombohedral, the tetragonal and a trace amount of orthorhombic phases, coexist in the MPB region ($0.28 \leq x \leq 0.40$). At the same time, the intensity of the tetragonal phase is enhanced with the increase of PT concentration. For $x \geq 0.5$, all the BDF- x PT samples show the pure tetragonal phase. Due to the lower stability of BiFeO_3 , some impurity phases, *i.e.* $\text{Bi}_2\text{Fe}_4\text{O}_9$ and $\text{Bi}_{25}\text{FeO}_{39}$, appear in the bismuth-rich compositions. However, the amount of the impurities is significantly diminished in the final ceramics after sintering at higher temperatures.

The crystal lattice parameters have been calculated for all the compositions, and their variations as a function of composition are shown in Fig. 2. For the compositions with rhombohedral phase, the volume of the (hexagonal) unit cell

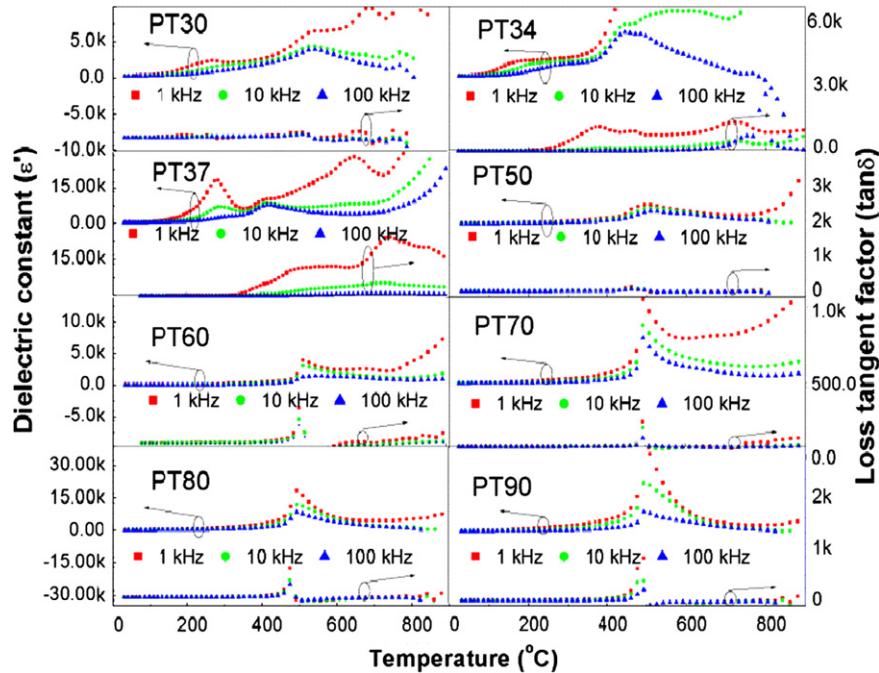


Fig. 3. Temperature dependences of the dielectric constant and loss tangent of the BDF- x PT ceramics measured at 1, 10, and 100 kHz.

increases from $x=0$ to $x=0.2$, which is caused by the substitution of ions with larger sizes on both A-site and B-site, i.e., $R(\text{Pb}^{2+}) > R(\text{Bi}^{3+}) > R(\text{Dy}^{3+})$, and $R(\text{Ti}^{4+}) > R(\text{Fe}^{3+})$, respectively [10,11]. For the compositions with tetragonal phase, the tetragonality, or c/a ratio, increases from 1.07 for $x=0.9$ to 1.16 for $x=0.4$ when approaching the MPB. Note that this highest value of c/a ratio for PT40 is almost the same as for the BF- x PT system [11]. The prominent tetragonality in the BDF-0.40PT ceramic mostly originates from the distortion of crystal lattice and the particular structural features near the MPB region.

Fig. 3 shows the temperature dependence of the dielectric properties in the BDF- x PT system, which appears to be very complicated because of the complex phase components and the electric conduction inherently present in BF-based materials. On the bismuth/dysprosium ferrite rich side from PT00 to PT20, the dielectric results (not shown) are meaningless at high temperatures because of the very large loss due to high conduction. On the lead titanate rich side from PT50 to PT90, one clear peak appears around 500 °C, which indicates the Curie temperature of the ferroelectric tetragonal phase to paraelectric cubic phase transition. In the MPB region, dielectric dispersion peaks appear around 200 °C, and other anomalies at 419 °C–534 °C, depending on composition.

According to the results discussed above, a preliminary phase diagram of the $(1-x)[0.9\text{BiFeO}_3-0.1\text{DyFeO}_3]-x\text{PbTiO}_3$ solid solution system is proposed, as shown in Fig. 4. Due to high losses, the phase transition temperatures for the samples of $0 \leq x \leq 0.20$ could not be determined by dielectric measurements. In Ref. [11], the T_C of 0.9BF-0.1DF was found to be about 320 °C, which is significantly reduced from the T_C of BF. Based on that, the

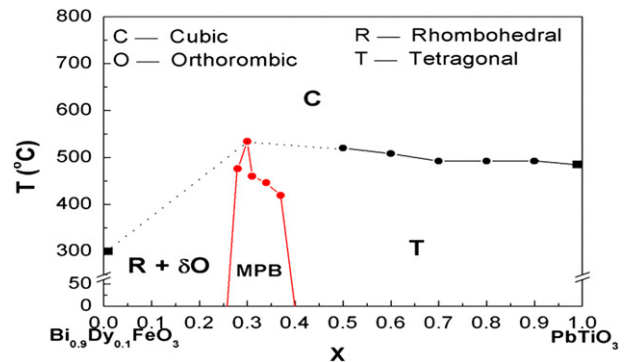


Fig. 4. Preliminary phase diagram of the $(1-x)\text{Bi}_{0.9}\text{Dy}_{0.1}\text{FeO}_3-x\text{PbTiO}_3$ solid solution (dashed lines indicate the expected trends).

T_C of the BDF- x PT system is expected to rise with the increase of PT concentration, as indicated by the dashed line in Fig. 4. The range of MPB ($0.28 \leq x \leq 0.40$, at room temperature) is narrowed down with the increase of temperature. For the compositions in the MPB region, the mixed phases (rhombohedral, tetragonal and orthorhombic) transforms to cubic phase at about 530 °C. For the compositions of $x \geq 0.5$, the tetragonal-cubic phase transition temperature changes slowly from 520 °C for PT50 to 492 °C for PT90.

The room temperature dielectric constant and loss tangent as a function of frequency are shown in Fig. 5. The dielectric constant and the loss tangent of the samples with $0 \leq x \leq 0.28$ decrease with the increase of frequency. In particular, for the samples in the MPB region, the dielectric constant is increased and almost remains the same value in the whole frequency range, as shown in Fig. 5(a).

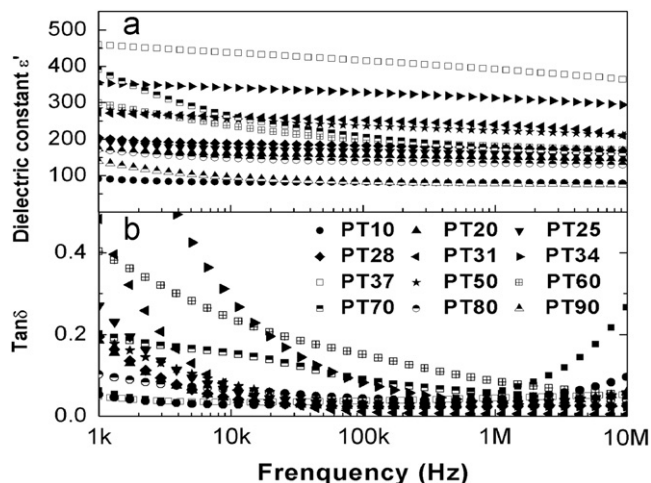


Fig. 5. Frequency dependences of (a) dielectric constant and (b) loss tangent of the BDF- x PT ceramics.

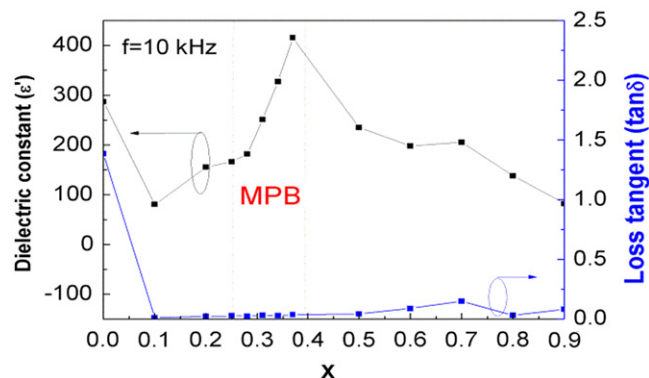


Fig. 6. Dielectric constant and loss tangent versus composition for the BDF- x PT ceramics.

In order to study the effects of PT substitution on the dielectric properties of the BDF- x PT pseudo-binary ceramics, the variations of the dielectric constant and loss tangent as a function of x PT, measured at 10 kHz, are plotted in Fig. 6. It can be seen that the dielectric constant increases with x increasing from 0.1 and reaches a maximum value of 437 at $x=0.37$, which can be related to the special structural feature in the MPB with the coexistence of rhombohedral, orthorhombic and tetragonal phase and multiple polarization state, making the materials more polarizable. In addition, the loss tangent value decreases significantly with the addition of a small amount of PT, as shown in Fig. 6, because of the formation of a more stable perovskite structure which has reduced the concentration of Fe^{2+} ions. Moreover, the loss remains low for the compositions in the MPB, while it increases slightly with the further increase of PT because of a lower quality of ceramics.

The synthesis, structure and dielectric properties of $(1-x)[0.9\text{BiFeO}_3-0.1\text{DyFeO}_3]-x\text{PbTiO}_3$ pseudo-binary solid solution system have been investigated. A continued solid solution of BDF-PT has been prepared. Based on the

structural analysis, a morphotropic phase boundary (MPB) region has been found in the composition range of $0.28 \leq x \leq 0.40$, in which the rhombohedral, tetragonal or orthorhombic phases coexist. The lead titanate-rich compositions show a large tetragonality with a c/a ratio reaching 1.16 in PT40 near the MPB. A preliminary phase diagram is proposed from the room temperature XRD and the temperature variable dielectric measurements up to high temperatures, which delimits the regions of the rhombohedral, tetragonal and cubic phases, as well as the MPB. The samples with compositions within the MPB region exhibit the best dielectric properties with the highest dielectric constant found in $x=0.37$. These results indicate that the formation of the BDF-PT solid solution and the existence of the MPB region contribute to the improvement of the stability of the perovskite phase and the enhancement of its dielectric properties.

4. Conclusions

The synthesis, structure and dielectric properties of $(1-x)[0.9\text{BiFeO}_3-0.1\text{DyFeO}_3]-x\text{PbTiO}_3$ pseudo-binary solid solution system have been investigated. A continued solid solution of BDF-PT has been prepared. Based on the structural analysis, a morphotropic phase boundary (MPB) region has been found in the composition range of $0.28 \leq x \leq 0.40$, in which the rhombohedral, tetragonal or orthorhombic phases coexist. The lead titanate-rich compositions show a large tetragonality with a c/a ratio reaching 1.16 in PT40 near the MPB. A preliminary phase diagram is proposed from the room temperature XRD and the temperature variable dielectric measurements up to high temperatures, which delimits the regions of the rhombohedral, tetragonal and cubic phases, as well as the MPB. The samples with compositions within the MPB region exhibit the best dielectric properties with the highest dielectric constant found in $x=0.37$. These results indicate that the formation of the BDF-PT solid solution and the existence of the MPB region contribute to the improvement of the stability of the perovskite phase and the enhancement of its dielectric properties.

Acknowledgments

This work was supported by the Natural Science Foundation of China (Grant nos. 50728201 and 90923001), the International Science & Technology Cooperation Program of China (Grant no. 2011DFA51880), the US Office of Naval Research (Grant nos. N00014-06-1-0166 and N00014-11-1-0552) and the Natural Science and Engineering Research Council of Canada. ZGY and WR also thank the “Changjiang Scholar Program” and the “Qianren Program” of the Chinese Government for support.

References

- [1] J.B. Neaton, C. Ederer, U.V. Waghmare, N.A. Spaldin, K.M. Rabe, First-principles study of spontaneous polarization in multiferroic BiFeO_3 , *Physical Review B* 71 (2005) 014113.
- [2] P. Fischer, M. Połomska, I. Sosnowska, M. Szymański, Temperature dependence of the crystal and magnetic structures of BiFeO_3 , *Journal of Physics C: Solid State Physics* 13 (1980) 1931–1940.
- [3] M.M. Kumar, V.R. Palkar, K. Srinivas, V. Suryanarayana, Ferroelectricity in a pure BiFeO_3 ceramic, *Applied Physics Letters* 76 (2000) 2764.
- [4] Y.P. Wang, L. Zhou, M.F. Zhang, X.Y. Chen, J.-M. Liu, Z.G. Liu, Room-temperature saturated ferroelectric polarization in BiFeO_3 ceramics synthesized by rapid liquid phase sintering, *Applied Physics Letters* 84 (2005) 1731.
- [5] S.T. Zhang, M.H. Lu, D. Wu, Y.F. Chen, N.B. Ming, Larger polarization and weak ferromagnetism in quenched BiFeO_3 ceramics with a distorted rhombohedral crystal structure, *Applied Physics Letters* 87 (2005) 262907.
- [6] V.A. Khomchenko, D.A. Kiselev, M. Kopcewicz, M. Maglione, et al., Doping strategies for increased performance in BiFeO_3 , *Journal of Magnetism and Magnetic Materials* 321 (2009) 1692–1698.
- [7] W.M. Zhu, Z.-G. Ye, Effects of chemical modification on the electrical properties of $0.67\text{BiFeO}_3-0.33\text{PbTiO}_3$ ferroelectric ceramics, *Ceramics International* 30 (2004) 1435–1442.
- [8] L. Chen, W. Ren, W.M. Zhu, Z.-G. Ye, P. Shi, X.F. Chen, X.Q. Wu, X. Yao, Improved dielectric and ferroelectric properties in Ti-doped $\text{BiFeO}_3\text{-PbTiO}_3$ thin films prepared by pulsed laser deposition, *Thin Solid Films* 518 (2010) 1637–1640.
- [9] W.-M. Zhu, Z.-G. Ye, Improved dielectric and ferroelectric properties of high Curie temperature $(1-x)\text{BiFeO}_3-x\text{PbTiO}_3$ ceramics by aliovalent ionic substitution, *Applied Physics Letters* 89 (2006) 232904.
- [10] W.-M. Zhu, H.-Y. Guo, Z.-G. Ye, Structural and magnetic characterization of multiferroic $(1-x)(\text{BiFeO}_3-x\text{PbTiO}_3)$ solid solutions, *Physical Review B* 78 (2008) 014401.
- [11] W.-M. Zhu, L.W. Su, Z.-G. Ye, W. Ren, Enhanced magnetization and polarization in chemically modified multiferroic $(1-x)\text{BiFeO}_3-x\text{DyFeO}_3$ solid solution, *Applied Physics Letters* 94 (2009) 142908.
- [12] Z.-L. Hu, Y. Wang, J.-Y. Dai, D. Zhou, Y.-M. Hu, H.-S. Gu, K.Z. Baba-Kishi, Enhanced multiferroic properties of La-doped BiFeO_3 nanotubes fabricated through anodic alumina template method, *Journal of Advanced Dielectrics* 1 (3) (2011) 325–330.